A comparative study of alkanolamines and inorganic additives on the microstructure development of blast furnace slag blended cement at low curing temperature.

Qi Zhai [a], Kiyofumi Kurumisawa [b, *], Juhyuk Moon [c]

[a] Division of Sustainable Resources Engineering, Graduate School of Engineering, Hokkaido University, Japan
[b] Division of Sustainable Resources Engineering, Faculty of Engineering, Hokkaido University, Japan
[c] Department of Civil and Environmental Engineering, Seoul National University, Korea

Abstract

The initial reactivity and strength development of blast furnace slag cement (BFSC) are crucial factors that increase its utilization. Therefore, it is important to select the most suitable accelerator. In this study, the impact of four accelerators, namely sodium sulfate (Na_2SO_4), calcium nitrite ($Ca(NO_2)_2$), triethanolamine (TEA), and diethanolisopropanolamine (DEIPA), on the hydration and strength development of BFSC at curing temperatures of 5 and 20 °C was investigated. Isothermal calorimetry, X-ray diffraction (XRD), scanning electron microscopy (SEM), and mercury intrusion porosimetry (MIP) were conducted. The results revealed that Na_2SO_4 effectively enhanced early age strength by accelerating the hydration of the clinker and slag. $Ca(NO_2)_2$ is sensitive to temperature changes. At 20 °C, $Ca(NO_2)_2$ promoted the reaction of the aluminates and slag in the initial stage. However, the presence of slag inhibited clinker hydration, and the addition of $Ca(NO_2)_2$ exacerbated this effect, resulting in reduced strength at 5 °C. Indeed, the use of TEA and DEIPA at 0.02% at 5 °C is not recommended. Complex interactions between TEA and Ca^{2+} may inhibit the formation of calcium hydroxide crystals, further inhibiting aluminate hydration. This may lead to low strength development at low curing temperatures such as 5 °C.

Keywords: Slag blended cement, Alkanolamine, hydration, calcium nitrite, sodium sulfate

1. Introduction

Ordinary Portland cement (OPC) is the most commonly used construction material worldwide, with an annual production rate of approximately 4 Gt. This substantial production contributes to approximately 10% of global CO_2 emissions [1]. To align with the Paris Agreement on Climate Change, it is imperative to reduce annual CO_2 emissions by at least 16% by 2030 [2]. Therefore, the development of clinker-free construction materials has attracted considerable attention. Currently, a significant portion of cementitious binders consist of blended Portland cement, which incorporates one or more supplementary

cementitious materials (SCMs) [3]. Ground-granulated blast furnace slag (GGBFS), hereafter referred to as slag, is a popular SCM that not only helps reduce CO_2 emissions but also decreases thermal energy consumption by approximately 1600 MJ/t [2].

Studies have indicated that slag-blended cement exhibits superior physical and chemical resistance compared with cement with an equivalent clinker replacement ratio [4], demonstrating higher compressive strength, enhanced durability, and increased resistance to corrosion in later stages [5]. Theoretically, the percentage of slag in the blended cement can reach 70% or higher. In practice, however, the recommended replacement ratio is limited to approximately 50% [6]. This limit is recommended owing to the stronger dilution effect of the cement at higher replacement ratios, which outweighs the positive filling effect of the slag [7]. The delayed reaction of the slag during the early stage of hydration explains this phenomenon. In the slag-blended cement, the slag remained largely unreactive until after 24 h [4]. Consequently, low reactivity and early strength development significantly restrict the achievable replacement ratio of slag in slag-blended cement, hindering its potential for higher levels of clinker replacement.

One promising approach for enhancing the early reactions of blast-furnace slag-blended cements is the addition of soluble organic compounds and inorganic salts [8]. Among these additives, Sodium sulfate (Na_2SO_4) is a well-known accelerator commonly used in slag-blended cement [9,10]. Numerous studies have demonstrated that Na_2SO_4 can significantly improve the compressive strength development at an early stage [11–13]. However, it is crucial to carefully control the dosage of Na_2SO_4, because excessive amounts may lead to reduced late strength owing to AFt recrystallization [14,15]. Calcium nitrite ($Ca(NO_2)_2$) is widely used as an anti-freezing agent and corrosion inhibitor in cement formulations owing to its non-chloride and alkali components [16,17]. It can also act as an accelerator by promoting the hydration of alite and tricalcium aluminate (C_3A). The formation of nitrite AFm ($Ca_3Al_2(OH)_{12}(NO_2)_2xH_2O$) is effective in accelerating the early strength development [18].

Alcohol amine monomers, such as triethanolamine (TEA) and diethanol-isopropanolamine (DEIPA), are commonly used as cement grinding aids because of their surface-active dispersion properties [18–21]. It has also been reported that alkanolamines can function as accelerators at low doses (< 0.1%) [22,23]. Several studies have shown that TEA can enhance the compressive strength of cement at the early stage when used at dosages of 0.02 to 0.05%. This promotion was attributed to the acceleration of aluminate hydration in both the early (formation of AFt) and late (formation of AFm) stages [21,24–26]. Liao et al. [24] found that TEA improved the early hydration of cement by accelerating aluminate hydration, although it may have prolonged the induction period because of its retardation effect on alite. This phenomenon was also confirmed by Zhang et al. [27], who observed that TEA can alter the morphology of portlandite by forming a TEA-Ca^{2+} complex. The intermixing of microcrystalline portlandite with C-S-H can result in an increased Ca/Si ratio. Xu et al. [21] found that the TEA-Ca^{2+} complex could further delay the hydration of alite by inhibiting portlandite growth. In addition, TEA has been found to promote the hydration and strength development of cement blended with cementitious materials. Tan et al. [28] investigated the effects of TEA on a cement-wet ground granulated blast-furnace slag system (WGGBS) and reported that TEA could increase the late strength by facilitating the formation

of a hydrotalcite-like phase. Huang et al. [29] indicated that TEA enhanced the strength of limestone-calcined clay cement, both in the early and late stages, by accelerating aluminate hydration and reducing porosity. Recently, as summarized by Lu et al. [26], TEA was shown to promote not only aluminate but also ferrite hydration, consequently affecting the hydration of alite. Despite considerable research into the effects of TEA on cement or blended cement hydration, limited information is available regarding its use in slag-blended cements. As a new type of alkanolamine, DEIPA is considered more environmentally friendly than TEA because of its low toxicity. DEIPA was also found to have a positive effect on hydration at an appropriate dosage. Riding et al. [23] reported that 0.02% DEIPA mixed with slag-blended cement could accelerate aluminate hydration and alter the morphology of portlandite. Ma et al. [20] observed this phenomenon and pointed out that DEIPA could enhance the formation of the AFt phase at the initial stage and subsequently promote the second hydration of the ferrite and aluminate phases. As reported by Wang et al. [30], 0.05% DEIPA can effectively increase the compressive strength of cement throughout the curing period with a more pronounced enhancement in the early stage.

Environmental conditions, particularly curing temperature, play an important role in cement-based material hydration [31–33]. The hydration and strength development of cement-based materials get significantly slower at low curing temperatures (0-10 °C). However, under low-temperature conditions, the basic hydration mechanism does not change noticeably, which may result in different properties compared to those exhibited by materials cured at ambient temperature [34,35]. For general applicability, it is important to further clarify and verify whether additives suitable at room temperature are also suitable at low temperatures.

In this study, the influence of two alkanolamines (TEA and DEIPA) at a low dosage compared with the commonly used inorganic salts Na_2SO_4 and $Ca(NO_2)_2$ on the slag-blended cement at curing temperatures of 5 and 20 °C was investigated. The objective of the investigation was to provide a better understanding of the influence of organic and inorganic additives on the hydration and strength development of slag-blended cements at different curing temperatures. The results of this investigation can be used to determine a more reasonable design for the replacement ratio of cement with chemical additives, and to provide some feasible suggestions for selecting the appropriate additives under the conditions of room and low curing temperatures.

2. Experimental

2.1.Raw Materials

All the cementitious materials used in this study were provided by Nippon Steel (Hokkaido, Japan). Commercial OPC and slag, which comply with the Japanese standards JIS R 5210 and JIS A 6206, respectively, were used. The specific surface areas of the OPC and slag were measured as 3260 and 3820 cm^2/g, respectively. The chemical compositions of the raw materials, as measured by XRF, are listed in Table 1. The mineral compositions of the raw materials are presented in Fig. A. 1 in the Appendix. Quartz powder (#300, MARUTOU, Japan) was used to obtain an inert filler with a size similar to that of the slag.

The particle size distributions of both materials are shown in Fig. A. 2. Analytical grade Na_2SO_4, $Ca(NO_2)_2{\cdot}H_2O$, TEA (Kanto Chemical, Tokyo, Japan), and DEIPA (Tokyo Chemical Industry, Tokyo, Japan) were used in this study. The OPC and slag were blended at a fixed ratio of 50:50, which is one of the most commonly used ratios in Japan, according to the JIS A 6206 standard. However, the sulfate content was not adjusted to accommodate the aluminate content present in the slag. To minimize bleeding, both mortars and pastes were prepared with a water-to-binder (OPC + slag) ratio of 0.4. The dosage of TEA and DEIPA was 0.02% by weight of the cement-slag binder, a value commonly used in previous studies [29,36,37]. Prior research has indicated that the optimal dosage of Na_2SO_4 in a 50:50 slag-cement binder is 1.0%-1.5% [11]. To ensure an observable effect without negatively affecting the later strength, a 1.0% binder dosage by weight was selected for Na_2SO_4. Similarly, a 1.0% dosage by weight of the binder was used for $Ca(NO_2)_2$ in this study, because it has been shown to promote the hydration of slag and cement in previous studies [16]. The mix designs of the slag-blended cement are summarized in Table 2.

Table 1 Chemical composition of slag, OPC and quartz powder (wt %).

Oxide	Slag	OPC	Quartz powder
CaO	41.8	66.88	0.03
SiO_2	33.8	20.48	95.79
Al_2O_3	13.3	5.06	2.32
MgO	7.2	1.50	0.07
SO_3	0.7	2.05	0.00
Fe_2O_3	0.7	2.89	0.11
TiO_2	0.5	0.29	0.06
Na_2O	0.4	0.22	0.12
K_2O	0.3	0.27	1.46
MnO	0.2	0.05	0.00
Others	0.1	0.01	0.3
LOI	0.46	2.5	0.35

Table 2 Mix proportions in this study.

Mix design	OPC (wt%)*	Slag (wt%)	Quartz powder**	Curing temperature	Additive (wt% of binder)
OPC	100	0			/
Blank					/
$Ca(NO_2)_2$					1.0%
TEA	50	50	0	“5 °C” “20 °C”	0.02%
DEIPA					0.02%
Na_2SO_4					1%
Blank	50	0	50		/

$Ca(NO_2)_2$	1.0%
TEA	0.02%
DEIPA	0.02%
Na_2SO_4	1.0%

* OPC was used only for the compressive strength tests.
** The samples mixed with quartz powder were only used for X-ray diffraction (XRD) and isothermal calorimetry testing within the initial two 2 d. This was done to isolate the impact of additives on the slag component within the slag-blended cement.

2.2.Mortar experiments

Mortar samples were prepared by mixing standard sand with a solid-to-liquid ratio of 2.5, to achieve the desired consistency. All the additives were dissolved in distilled water the day before mixing to ensure sufficient dissolution. Initially, the OPC, slag, and standard sand provided by the Japan Cement Association, compliant with JIS R5201 (density:2.64 g/cm^3, water absorption rate:0.42%, D90:0.16 mm), were premixed in a 5 L stirring mixer for 1 min to ensure homogeneity. After premixing, the solution was mixed with the solids for 90 s at low speed. To maintain homogeneity, the binders adhering to the blades and edges of the bowl were scraped using a spatula for 30 s, followed by high-speed mixing for 120 s. Once the mixing was complete, fresh mortar was immediately poured into a cylindrical mold (50-mm in diameter and 100-mm in length) and sealed with plastic sheets. The mortar samples were then stored in curing chambers with 98% relative humidity at 5 and 20 °C, respectively.

After curing for 3,7 and 28 d, the samples were demolded, and the compressive strength was measured, with an average value calculated from three samples.

2.3.Paste preparation

The solution containing the chemical additives mixed with distilled water was left overnight at 20 °C to ensure sufficient dissolution. Before adding the solution, the anhydrous cement and slag were mixed in a 2.5 L mixer to achieve homogeneity. After adding the required amount of solution, the mixture was gently homogenized for 90 s, followed by a 30-second pause with intermittent scraping using a spatula to maintain homogeneity. Finally, the mixture was combined for 2 min at high speed. The paste was cast into a plastic cup with a diameter of 50 mm and length of 50 mm, which was covered with plastic sheets. The samples were then cured at 5 and 20 °C.

After the specified curing periods of 3 and 28 d, the samples were demolded. To investigate the effects of the additives during the fresh stage, samples for XRD testing were collected at various time intervals ranging from 2 h to 20 h before the one-day mark (specifically at 2, 6, 10, 12, 16, and 20 h) based on the isothermal calorimetry test. The outer layer of each sample was then removed. For scanning electron microscopy (SEM) observation, the samples were cut into 3-5 mm discs using a diamond saw, and the remaining portion was crushed with a hammer and sieved to obtain particles ranging in size from 2 to 5 mm. Hydration was stopped by replacing the solvent with acetone, as described in a previous study [38]. Subsequently, the acetone was decanted, and the specimens were dried in a

constant curing chamber at 40 °C for 1 d. The samples for XRD analysis were further ground into powder with a particle size of less than 300 μm. All the samples in which hydration was stopped were stored in vacuum bags until further analysis.

2.4.Paste experiments

2.4.1. Isothermal calorimetry

The generated heat was monitored using an isothermal calorimeter MMC-5116 (Tokyo Riko) instrument set at 5 °C for 14 d and 20 °C for 7 d. Before each experiment, the calorimeter was recalibrated and left for 1 d to maintain stability, and the glass ampoules were stored at the corresponding temperature overnight until the experiment. To investigate the influence of additives on the slag in slag-blended cement, 10 g of cement was mixed with 10 g of quartz powder. Because the internal mixing method in the calorimeter could not yield a homogeneous mixture, approximately 20 g of the binder was blended by hand outside the calorimeter for 5 min [4]. The samples were then immediately placed in a calorimeter.

2.4.2. SEM observation

The reaction degree of the slag and hydration degree of the clinker were calculated based on backscattered electron (BSE) images [39]. For BSE observation, 3-5 mm discs were impregnated with epoxy resin and left to harden for 1 d, followed by drying at 40 °C for at least 3 d. To create a mirror surface suitable for Scanning Electron Microscopy with Energy-Dispersive X-ray Spectroscopy (SEM-EDX) measurements, the impregnated disc surface was sequentially polished down to 1 μm using ethanol as a lubricant. The specimen was then coated with Pt to increase its electrical conductivity. SEM-EDX measurements were performed using a JEOL JSM-IT200 scanning electron microscope equipped with an EDX detector. The electron acceleration voltage used to operate the microscope was 15 kV, and the working distance was approximately 10 mm. Images were collected at 500x. Two samples and 20 images were analyzed. The degree of reaction between slag and cement was calculated as follows [40]:

$$\alpha = 1 - \frac{V_i}{V_0}, \quad (1)$$

where V_0 is the initial fraction of the solid in the binder and V_i is the unreacted slag or unhydrated cement at age i.

2.4.3. Powder X-ray diffraction

XRD data were obtained using a MultiFlex diffractometer to characterize the phase assemblage during hydration and quantify the crystalline phase. The diffractometer was equipped with a Cu-Kα X-ray tube and measurements were run at 40 kV and 40 mA in the angular range of 5–70° (2θ). The scan was conducted in steps of 0.02°, for 1.2 s per step. To the samples, corundom (α-Al_2O_3) was added at 20% wt as an internal standard to quantify the amount of amorphous phase. The XRD data were analyzed using the Profex software with Rietveld refinement. The amounts of C–(A)-S-H and unreacted slag were determined from the BSE results.

2.4.4. Morphology observation

Prior to the observation, the discs were directly coated with Pt and stored in a vacuum desiccator. Morphological analysis was carried out using FE-SEM (JEOL JSM-7200F), equipped with EDS (JEOL, EX-94300S4L1Q), operated in the Secondary Electron (SE) mode. Qualitative point studies were conducted to identify the chemical composition of the specific phases. The observations were performed at a voltage of 15 keV and a working distance of 10 mm.

2.4.5. Mercury intrusion porosimetry (MIP)

Mercury intrusion porosimetry was conducted using a Micromeritics Auto Pore V 9600 instrument to evaluate the porosity and pore size distribution of the paste samples. After loading a sample into a low-pressure station, the glass cell was filled with Hg. Low-pressure analysis was performed up to 50 psia. A high-pressure analysis was performed at pressures between 50 and 60,000 psia. The contact angle was set to 130°, and the surface tension was set to 0.485 N/m.

3. Results and discussion

3.1.Compressive strength

Figure 1 illustrates the influence of the chemical additives on the compressive strength of the mortars. Figure 1a presents the development of compressive strength of mortars cured at 5 °C. Na_2SO_4 demonstrated superior promotion from 3 to 28 d, whereas $Ca(NO_2)_2$ only exhibited an acceleration effect at 28 d. TEA showed a slight promotional effect at 7 d, with a 20% increase compared to the control group. By contrast, similar to the behavior of mortars treated with DEIPA and cured at 5 °C, the strength of the samples treated with DEIPA and cured at 20 °C was also inhibited for up to 28 d (Fig. 1b). However, the samples treated with other additives and cured at 20 °C showed a completely different trend.

The addition of Na2SO4 and $Ca(NO_2)_2$ promoted strength development up to 7 d, with the Na_2SO_4-treated sample showing more strength gain at 3 d, indicating the beneficial role of alkalis in enhancing the early compressive strength in slag-blended systems, as reported in the literature [11,12]. However, no significant increase in strength was observed in the samples treated with alkanolamines at low dosages throughout the entire period, which differed from the behavior observed in OPC systems or OPC blended with other supplementary cementitious materials (SCMs). At 28 d, the slag-blended cement without any additives surpassed all the other samples, showing comparable or even higher strength than OPC with the same water-to-binder ratio. This can be attributed to the high slag reactivity at 28 d, which is further explained in the following section. Among the additives, Na_2SO_4 exhibited the highest decrease in strength, which was 22% less than that of the control group, whereas DEIPA showed only a 4% decrease, representing the smallest decline in strength.

In general, the effect of additives on strength development is highly susceptible to the influence of curing temperature. From the point of view of improving early strength, Na_2SO_4 showed a significant promotion effect at curing temperatures of both 5 and at 20 °C. $Ca(NO_2)_2$ was more suitable for use at 20 °C. TEA and DEIPA did not perform well in this study, and even exhibited an inhibitory effect on strength compared to the control group.

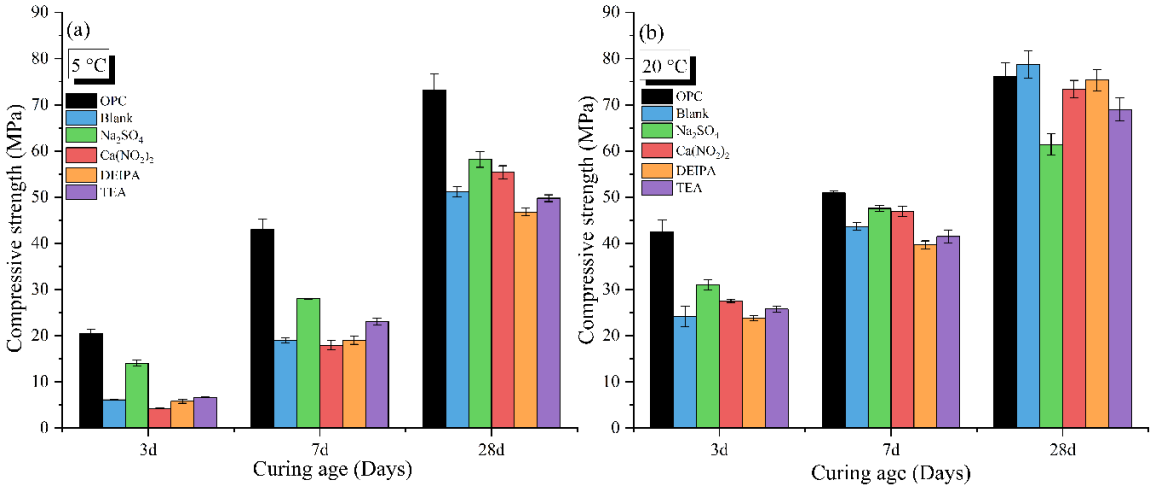

Fig. 1. Compressive strength of slag-blended cement mortars containing chemical additives. a) cured at 5 °C; b) cured at 20 °C.

3.2.Total hydration degree of clinker and reaction degree of slag

The total degree of clinker hydration and the reaction degree of the slag were obtained from the BSE images, as shown in Fig. 2. The curing temperature had an extremely strong influence on the hydration of the early cement clinker, with the low-temperature curing conditions creating an inhibitory effect on the hydration of the clinker (Fig. 2a). However, the effect on the subsequent cement clinker hydration was not significant. By contrast, except for the sample with $Ca(NO_2)_2$, low-temperature curing did not affect the reactivity of the slag in the early stage, but had a strong effect in the later stage (Fig. 2b). This may be due to the low reactivity of slag during the early stage. The total hydration of the clinker under all conditions in the later stage was very similar at approximately 70%. The effect of $Ca(NO_2)_2$ was sensitive to the curing temperature. Except for $Ca(NO_2)_2$, all the other additives promoted the reaction of slag and the hydration of the clinker at 3 d, irrespective of the curing temperature. Na_2SO_4 exhibits the greatest promotional effect. No difference in the degree of hydration of the clinker was observed at 28 d, irrespective of the curing temperature. The effects of additives on the specific components of the clinker are described in the next section. Figure 3 illustrates the correlation between strength development and the reaction degree of the binder. As shown in the figure, a positive relationship is observed. The enhancement in the compressive strength was linked to the augmentation of the degree of reaction between the clinker and slag.

BSE images of the samples at 3 d were selected and are presented in Fig. 4. Compared to the samples cured at 20 °C, the lower curing temperature appeared to result in a coarser microstructure, as indicated by the presence of black-hole-like areas in the corresponding images (Figs. 4a, c, e). In the case of Na_2SO_4, a denser C-(A)-S-H ring, highlighted by the yellow oval, was observed around the unhydrated clinker (Fig. 4b), compared with other samples at 20 °C. As shown in Figs. 6d and f, the presence of TEA and DEIPA resulted in the formation of thin plates, such as portlandite. TEA and DEIPA have the capability to form complexes with Ca^{2+} via chelation. These complexes may contribute to the growth of

portlandite, attributed to portlandite microcrystals [27,41]. Two other phenomena are noteworthy. Although the amount of microcrystalline portlandite seems minimal, this phenomenon can probably be attributed to Na2SO4 (Fig. 4b). This has been previously reported for white cement-slag systems with Na_2SO_4 [12]. Another new finding is that TEA, in addition to causing the microcrystallization of portlandite, seems to produce many needle-like carbonates around the portlandite cluster, as detected by EDX (Figs. 4d and f).

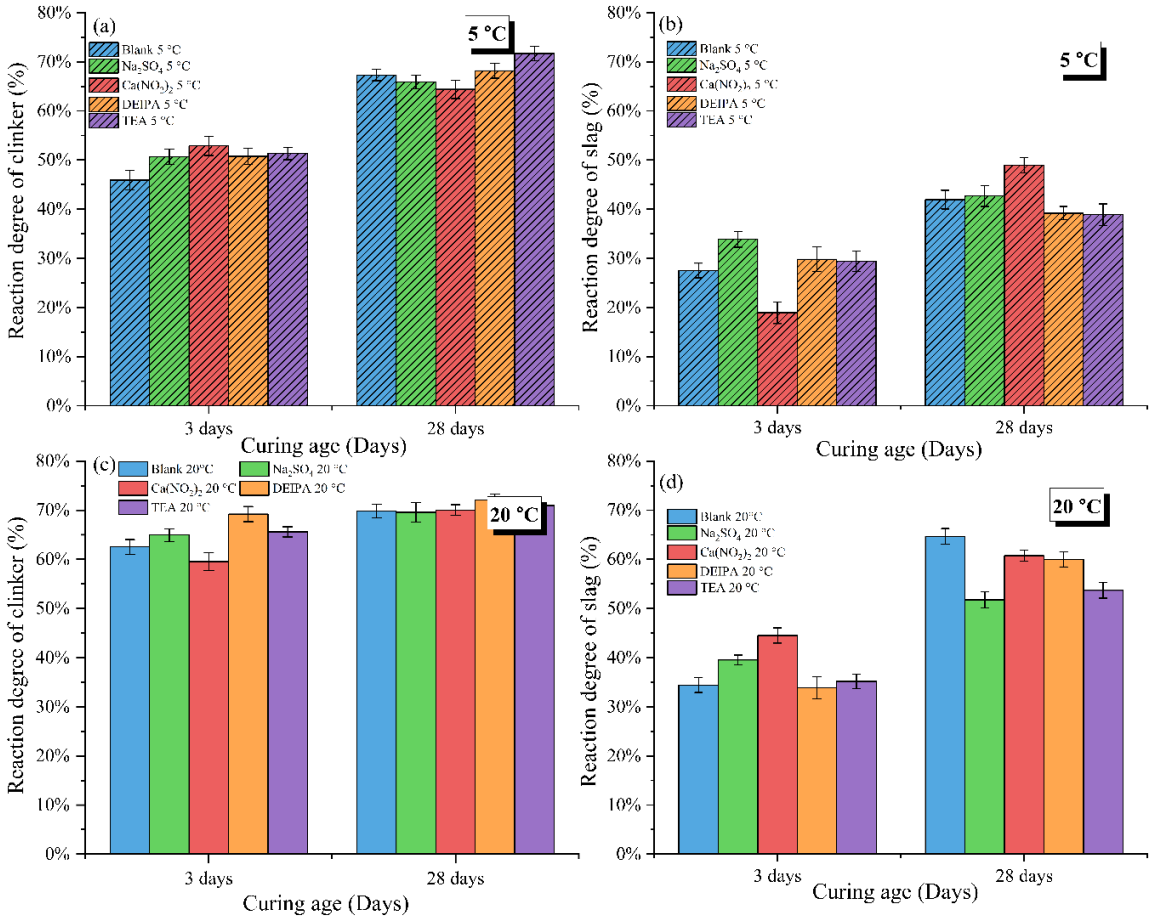

Fig. 2. The degree of reaction of slag and clinker up to 28 d by BSE. a) clinker cured at 5 °C, b) slag cured at 5 °C, c) clinker cured at 20 °C and d) slag cured at 20 °C.

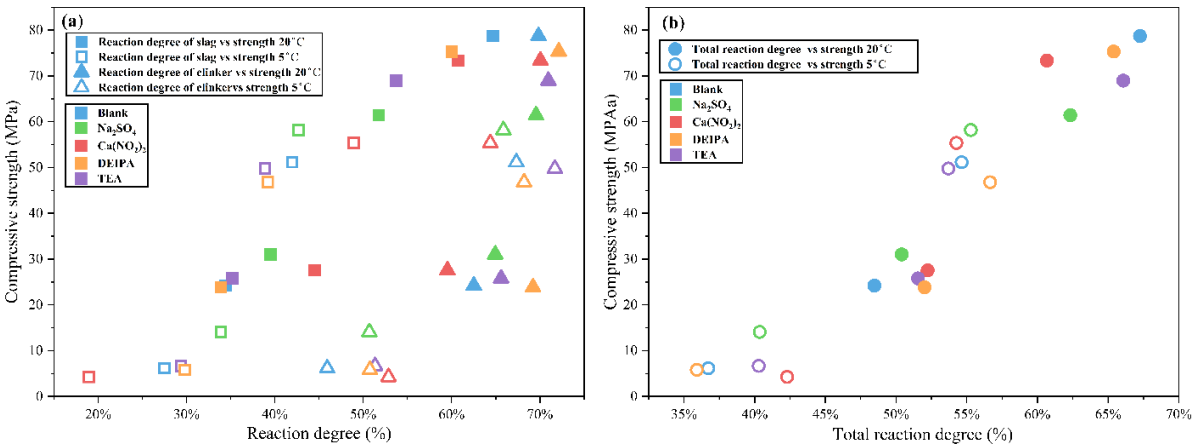

Fig. 3. Relationship between compressive strength and reaction degree of the binder.

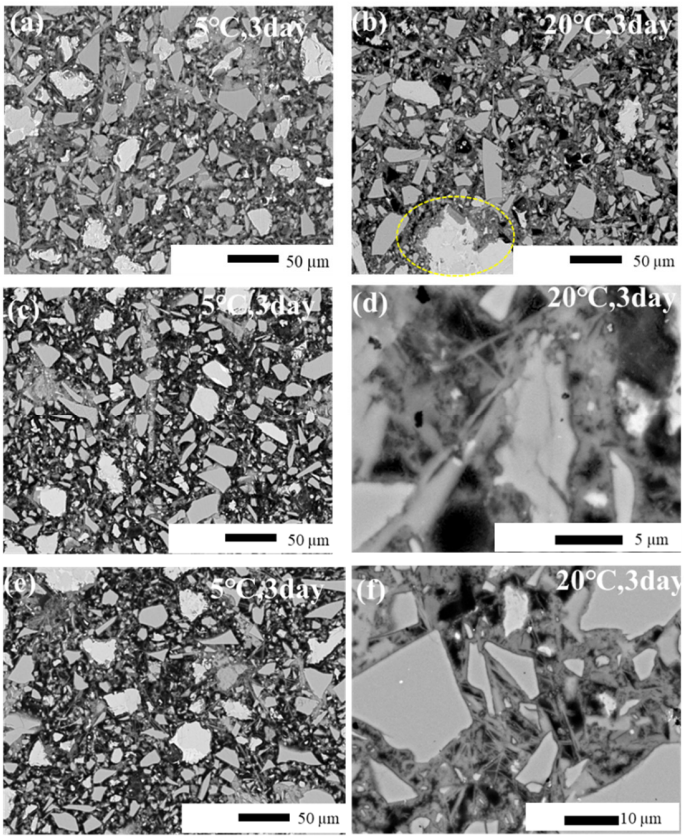

Fig. 4. Microstructure of slag-blended cement observed by BSE.

3.3.Hydration phase assemblage

The XRD results are presented in Fig. 5. As shown in Figs. 5a and b, the main crystalline hydrates identified were AFt, portlandite, monocarboaluminate, hemicarboaluminate, and monosulfate. Lower curing temperatures hindered the phase transformations of

monocarboaluminate and hemicarboaluminate.

The quantitative XRD results are shown in Fig. 6. After 3 d, the additives accelerated the hydration of alite and belite at 5 °C, resulting in the formation of more C-(A)-S-H compared to the control group. Specifically, Na2SO4 facilitates the rapid hydration of alite, leading to the formation of a significant amount of C–(A)–S-H, which accounts for 28% of the total weight. However, during the three-day hydration period at 20 °C and the 28-day hydration period, the additives did not have a significant impact on the phase assemblage. Notably, the amount of C-(A)-S-H produced at 28 d was comparable to or even exceeded the amount in the sample with additives, depending on the curing temperature. This phenomenon may explain the higher compressive strength of the control group. Both TEA and DEIPA promoted the hydration of the ferrite phase throughout the entire duration of this study. This effect can be attributed to the ability of TEA and DEIPA to form complexes with Fe, thereby increasing the mobility of Fe in the pore solution [19,22].

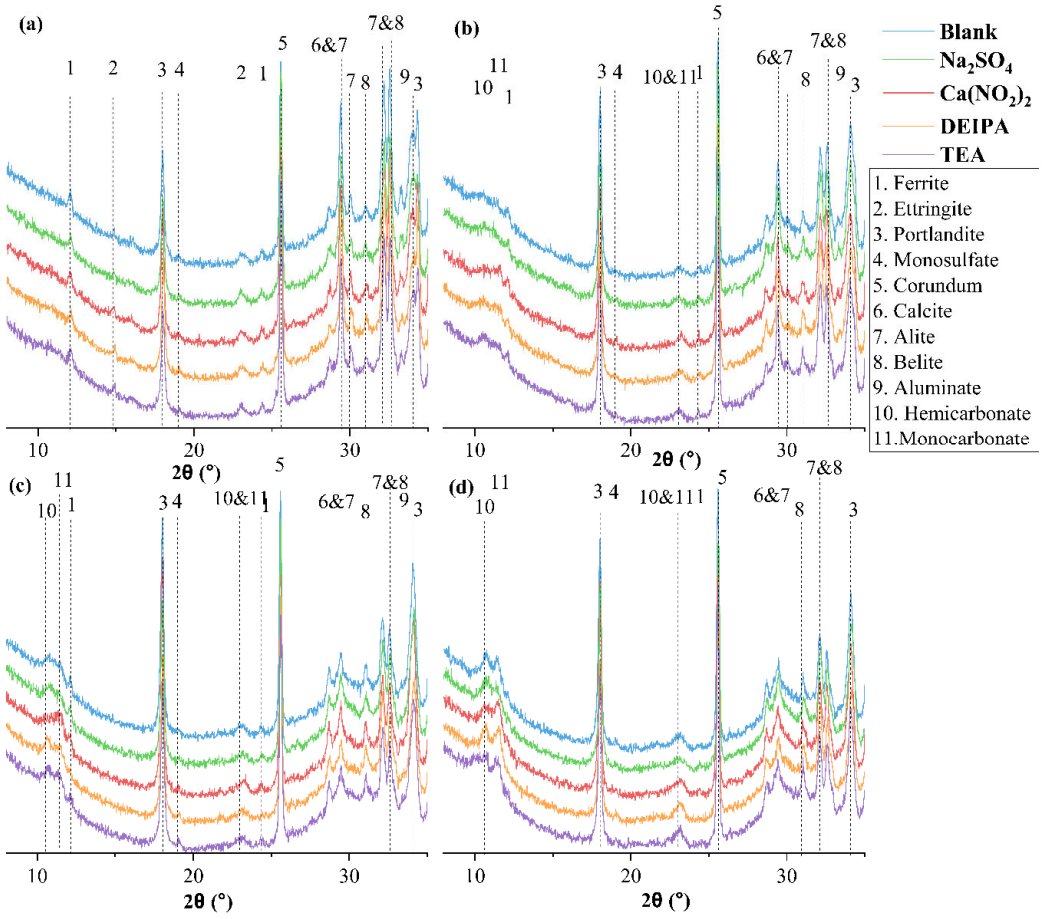

Fig. 5. XRD spectra of pastes treated with additives. a) 3 d cured at 5 °C; b) 3 d cured at 20 °C; c) 28 d cured at 5 °C and d) 28 d cured at 20 °C.

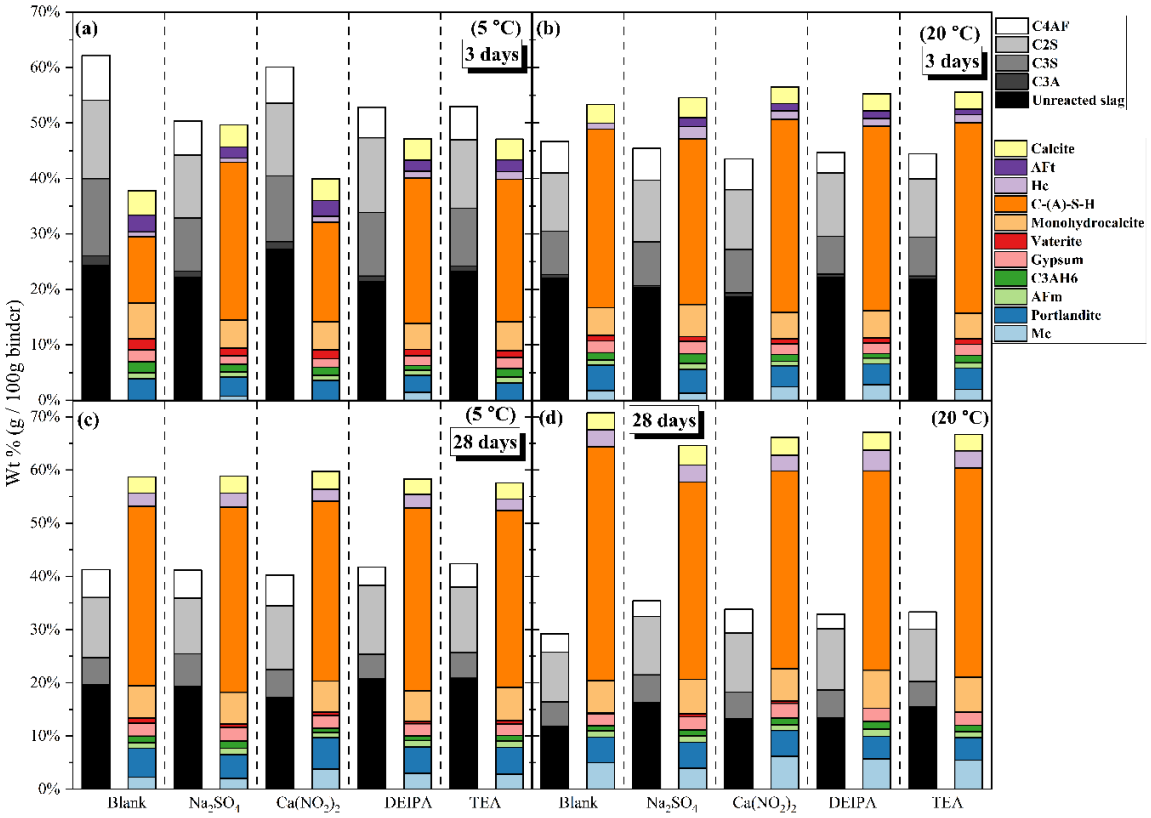

Fig. 6. Phase assemblage of samples treated with chemical additives. a) 3 d cured at 5 °C; b) 3 d cured at 20 °C; c) 28 d cured at 5 °C and d) 28 d cured at 20 °C.

3.4.MIP

At 3 d, Na_2SO_4 demonstrated significant effectiveness in reducing the porosity of the hardened paste at both 5 and 20 °C, as depicted in Figs. 7a and c. The samples containing Na_2SO_4 exhibited the smallest critical entry radius and the lowest total porosity at 5 °C, as shown in Fig. 7b. By contrast, the other additives did not show a significant refinement effect on the pore structure at 5 °C, as they all displayed similar total porosity and critical entry radius values (approximately 758 nm). However, at 20 °C, DEIPA, TEA, and $Ca(NO_2)_2$ reduced the volume of the pores larger than 300 nm. Notably, $Ca(NO_2)_2$ showed a pronounced effect at 20 °C, as the peak shifted to 60 nm, which is consistent with the observed strength development. This refinement effect is considered beneficial for enhancing strength [29].

After 28 d, the pore characteristics of the samples treated with TEA and DEIPA were similar to those of the control group. The critical pore entry radii were approximately 54 and 9 nm at 5 and 20 °C, respectively (Figs. 8a and c). However, at this stage, the negative impact of Na_2SO_4 on the formation of large pores was significant. The total porosity of the Na_2SO_4-treated samples was 4% and 7% higher than that of the control group at 5 and 20 °C,

respectively. This effect was relatively mild under low-temperature curing conditions, possibly owing to the slower hydration rate, which allowed sufficient time for pore structure refinement. The $Ca(NO_2)_2$ continued to refine the pore structure, particularly at low curing temperatures. This refinement effect may be related to the low degree of reaction at the early stage, indicating that the late reaction of the slag could be promoted (Fig. 2). A strong linear inverse correlation was observed between the capillary porosity and compressive strength, as shown in Fig. 9. This finding suggests that strength development was caused by the coarse-pore-filling of the reaction products.

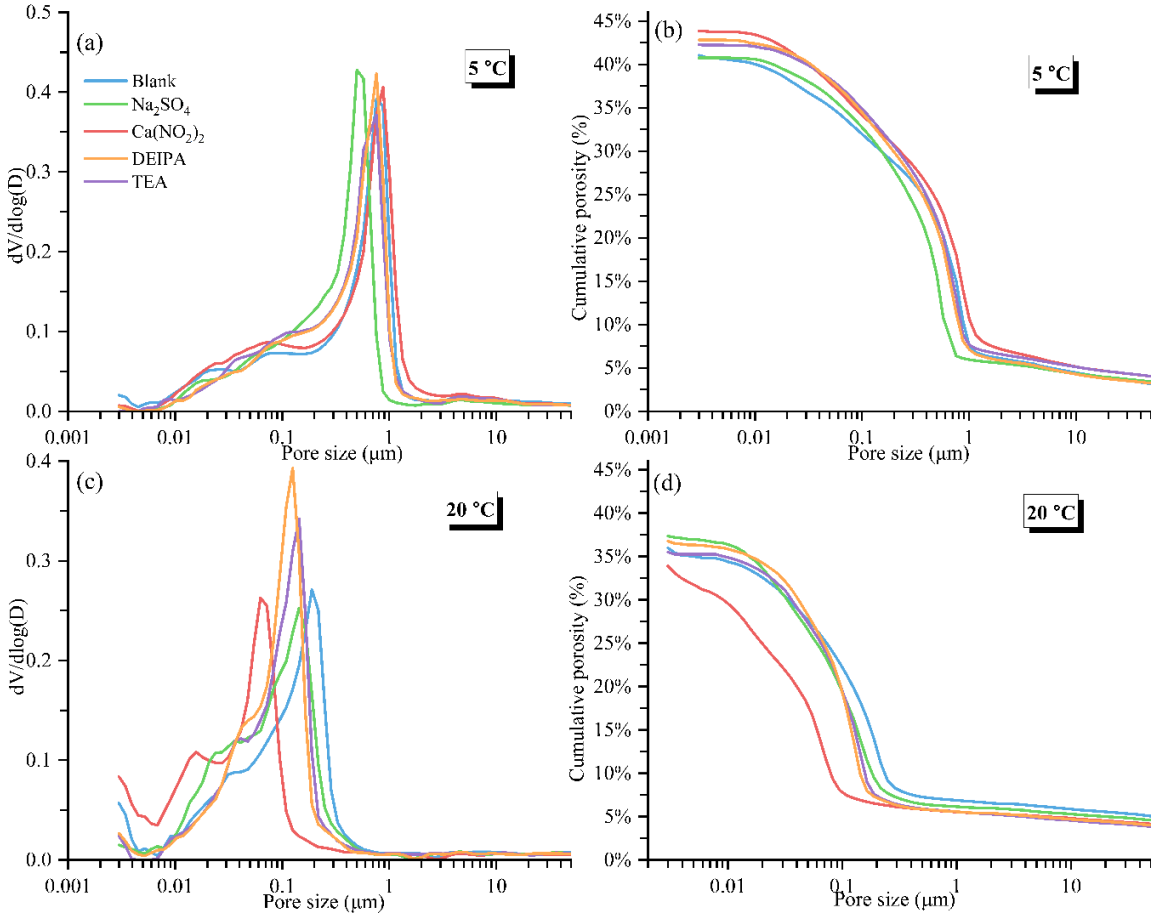

Fig. 7. Pore structure of the pastes treated with chemical additives at 3 d. a) and b) pore size distribution of the samples cured at 5 °C; c) and d) pore size distribution of samples cured at 20 °C.

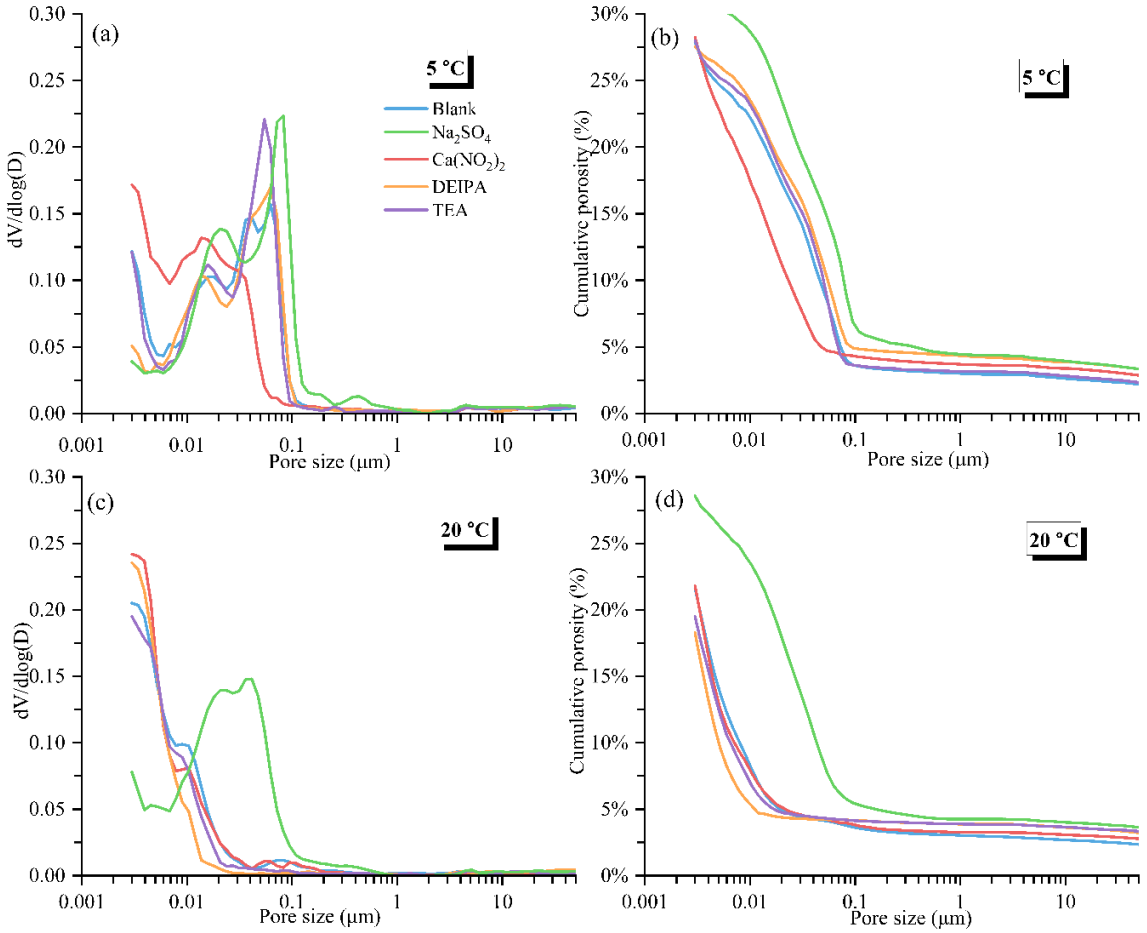

357

358 Fig. 8. Pore structure of the pastes treated with chemical additives at 28 d. a) and b) pore size
359 distribution of the samples cured at 5 °C; c) and d) pore size distribution of samples cured at
360 20 °C.

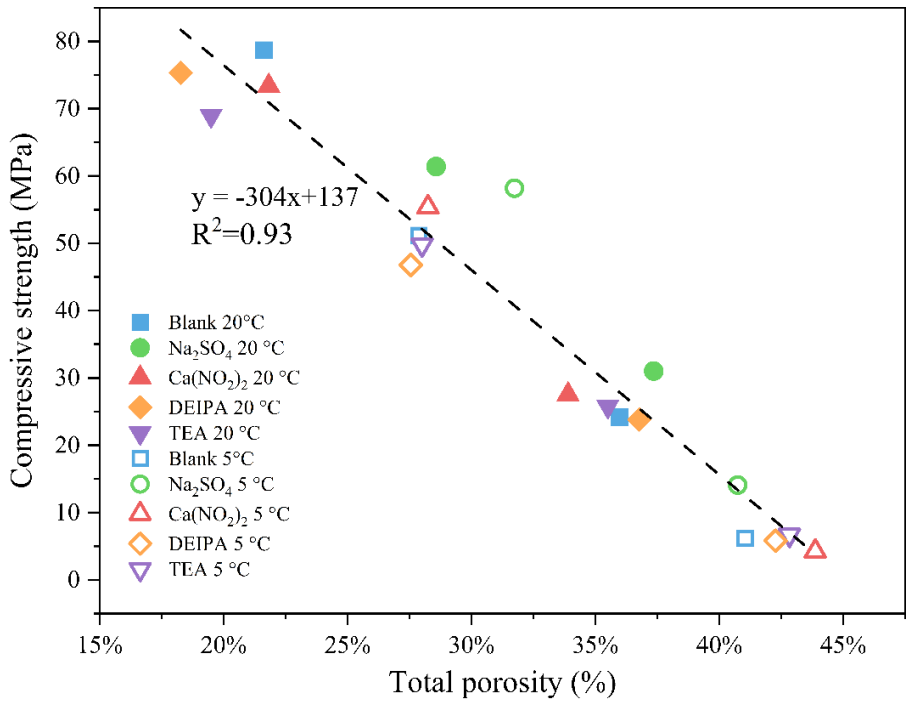

Fig. 9. Relationship between compressive strength and capillary porosity.

3.5.Morphology

Figure 10 shows the morphologies of the samples cured for 3 d. Except for TEA (Fig. 10e), the presence of the additives did not induce significant changes in the morphology. In the control group (Fig. 10a), needle-like C-(A)-S-H was observed attached to the surface of the unreacted slag [42]. The samples containing Na_2SO_4 and DEIPA (Figs. 10b and d) exhibited numerous hexagonal plate-like phases, which were identified as the AFm phase. In the case of DEIPA, in addition to hexagonal plates, such as the AFm phase, needle-like C-(A)-S-H and sheet-like AFm phases were also observed. By contrast, the samples containing TEA displayed a distinct morphology characterized by the presence of numerous flower-like or petal-like hydration products. EDX analysis confirmed that these products were carbonates. It is important to mention that all samples underwent the same curing conditions, indicating that TEA could potentially influence calcite stability.

The influence of TEA on the morphology of slag-blended cement was further investigated, as shown in Fig. 11. The curing temperature did not significantly affect the morphology. On day three, petal-like carbonates were generated (Figs. 11a and c). At 20 °C, it can be observed that some carbonates mixed with the needle like C-(A)-S-H, and a large amount of plate-like phase was attached at the surface of unreacted slag (Fig. 11c), which may be the reason for the further inhibition of slag reaction. At later ages, petal-like carbonates were not clearly observed; instead, silk- and cluster-like phases were generated. As verified by EDS, both were carbonates, which further confirmed that TEA caused structural changes in the carbonates. As suggested by previous studies, the stability of

carbonates is significantly affected by temperature, pH, Mg concentration, and organic additives (amines and alcohols, etc.) [43]. The ability of amines to form chelates with calcium ions may lower the concentration of free ions, which induces structural changes in the carbonate [44]. As chelate formation of the TEA-Ca^{2+} complex is well observed in cement with the TEA system at the same dosage of TEA, we believe that the TEA-Ca^{2+} complex could also form in slag-blended cement [27].

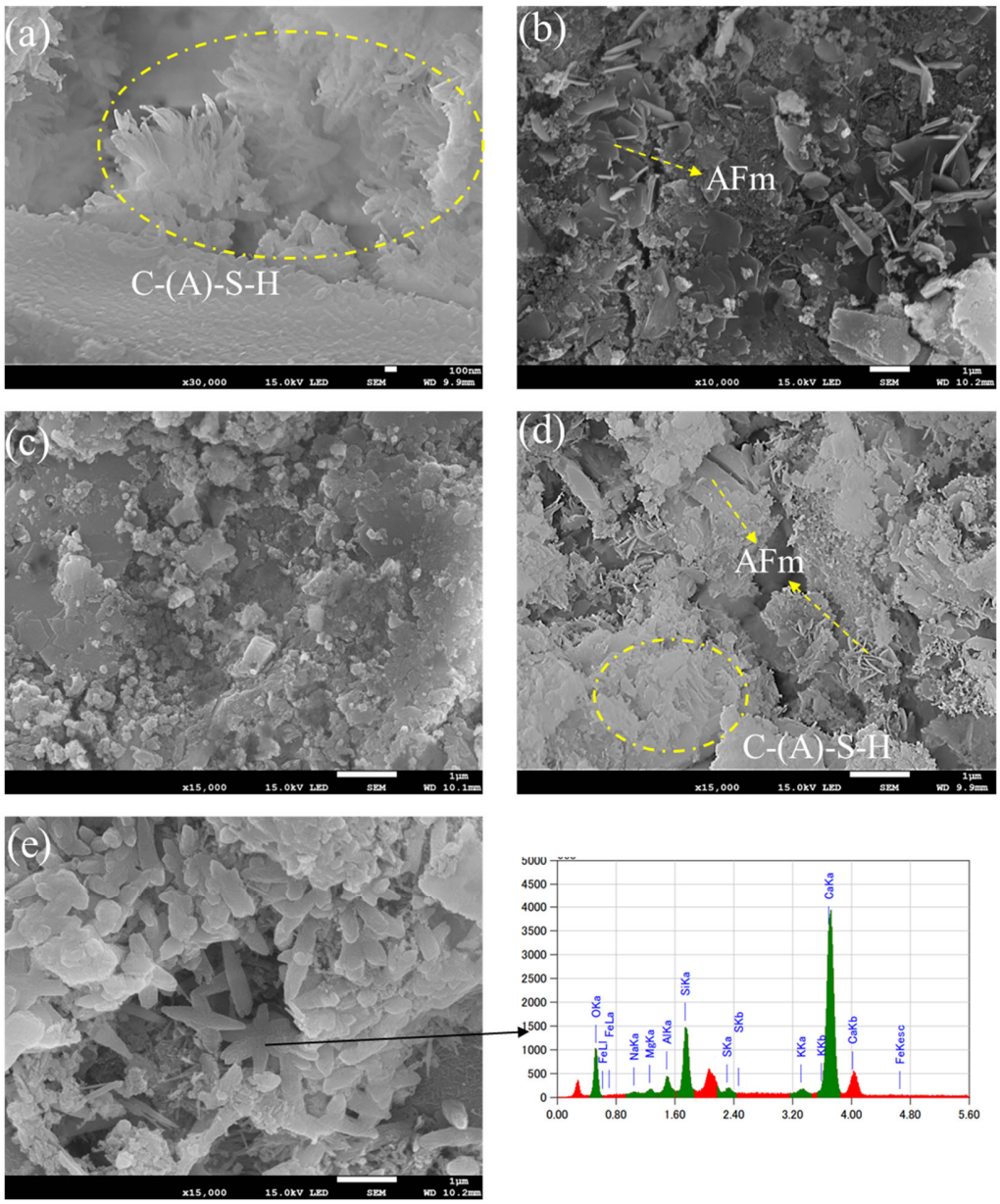

Fig. 10. Morphology of the slag blended cement at 3 d. a) Blank; b) Na_2SO_4; c) $Ca(NO_2)_2$; d) DEIPA; e) TEA.

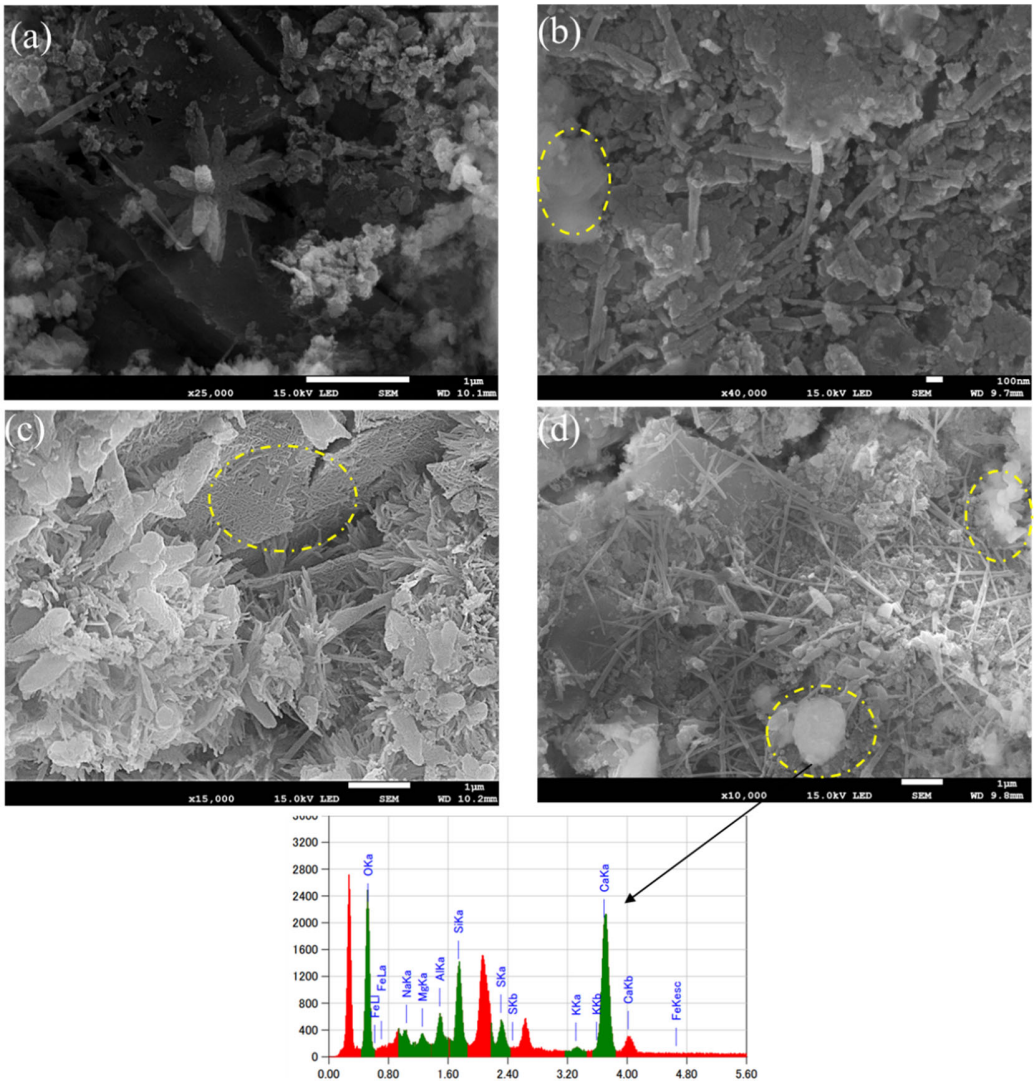

Fig. 11. The influence of TEA on the morphology of slag-blended cement cured at a) 5 °C at 3 d; b) 20 °C at 3 d; c) 5 °C at 28 d; d) 20 °C at 28 d.

3.6.Early stage of hydration

Figure 12 shows the heat generated by the pastes. The associated phase assemblages are summarized in Fig. A. 4. The additives significantly affect the hydration kinetics of the paste. However, the developmental trends of the additives were significantly different. The Na_2SO_4 stimulated the heat generation and exhibited the largest cumulative heat value (Figs. 12b and d). During the hydration process, a notable exothermal peak occurred, which combined with the main and secondary hydration peaks owing to the rapid consumption of gypsum (Fig. A. 4) [11]. During the deceleration period, heat production dropped sharply. For $Ca(NO_2)_2$, the main hydration peak occurred rapidly approximately 5 h after hydration (Fig.

12c) and highly accelerated the hydration of alite (Fig. A. 4). Compared to the other samples, the peak during the main hydration period was narrower and sharper, which may be due to the low amount of precipitated portlandite. TEA and DEIPA had significant effects on the hydration kinetics. Both TEA and DEIPA slightly prolonged the induction period and induced an earlier sulfate depletion peak (Figs. 12a and c). With the addition of TEA and DEIPA, the main hydration peaks became sharper and more intense (Fig. 12c). However, as shown in Fig. 12d, the total cumulative heat of the samples treated with TEA and DEIPA showed no significant changes compared to the control group. In addition to the additives, the curing temperature also significantly affected the heat release of the pastes. Low curing temperatures had a pronounced inhibitory effect on the exothermic reactions and delayed the period of heat generation, as illustrated in Fig. 12a. Most of the samples with additives exhibited a similar trend in cumulative heat development compared to those cured at 20 °C. However, the sample with $Ca(NO_2)_2$ exhibited a notable deviation, particularly after 30 h, with the lowest cumulative heat. This may be attributed to the inhibition of aluminate hydration by $Ca(NO_2)_2$. This further indicates that the effects of $Ca(NO_2)_2$ are highly influenced by the curing temperature. As shown in Fig. 13, the shapes and amplitudes of the slag- and quartz-containing samples are similar, which indicates that the additives primarily affect the initial stage of cement hydration. The influence of the curing condition changes on the slag reaction is further investigated in the next section.

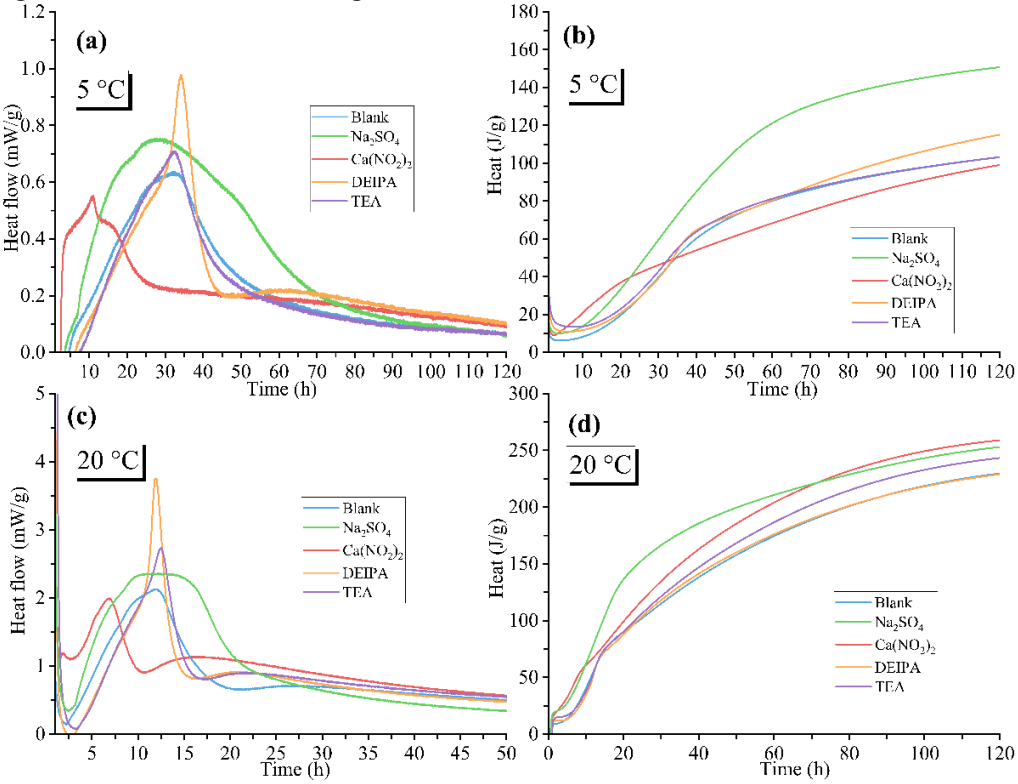

Fig. 12. Effect of additives on the heat flow and cumulative heat of slag-blended cement a) and b) 5 °C; c) and d) 20 °C.

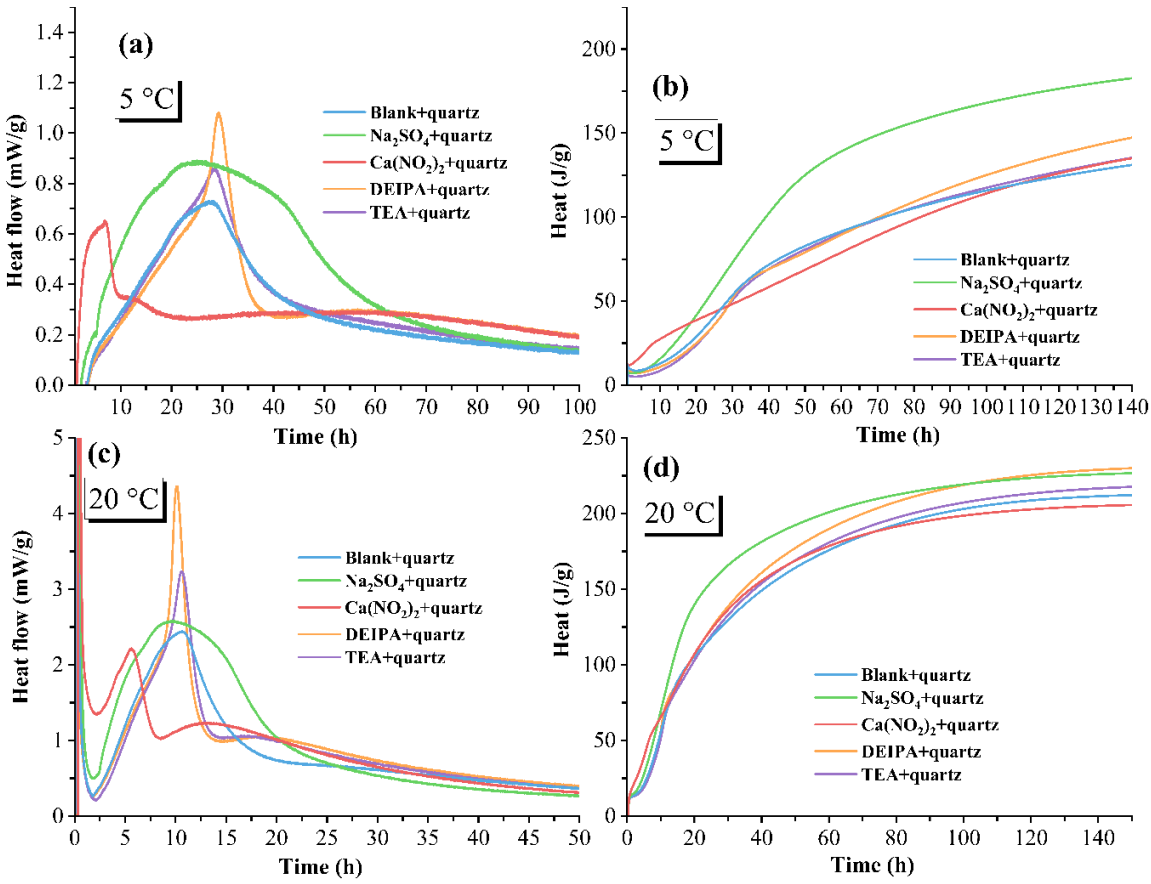

Fig. 13. The influence of additives on the heat flow and cumulative heat of cement treated with quartz powder a) and b) 5 °C; c) and d) 20 °C.

3.7.Mechanisms of effects of the additives on slag reaction

The above sections show the different effects on the properties of slag-blended cement systems. To clarify the mechanisms underlying the inhibitory and promotional effects of the additives, the fresh state of hydration was further investigated.

To distinguish between cement hydration and slag reaction, the difference between the slag-blended cement and quartz-blended cement systems was obtained using the following subtraction method [4]:

$$\Delta Q_t = Q_{quartz,t} - Q_{slag,t}, \quad (2)$$

where ΔQ_t is the difference in heat release between the slag-blended cement and quartz-blended cement at time t, $Q_{quartz,t}$ is the heat release in the presence of quartz at time t, and $Q_{slag,t}$ is the heat release in the presence of slag at time t. It should be noted that the reaction of the pastes in the calorimeter can cause water evaporation, leading to certain observed phenomena that may not align with other experimental results. However, these results provide reference values to a certain extent.

Figure 14 shows the difference between samples treated with slag and quartz powder and cured at 20 °C. The results for samples cured at 5 °C are shown in Fig. A. 3 in the appendix. Some differences were observed between the samples with and without quartz powder before the crossover point, which represented the starting point for the contribution of the slag reaction to the cumulative heat. Quantitative XRD analysis (Table B. 1) revealed that the clinker in the cement samples treated with quartz powder exhibited a higher degree of hydration. This difference may be attributed to a slight disparity in the particle size between the quartz powder and slag (Fig. A. 2), with quartz powder having a smaller particle size and acting as an effective filler. As indicated by the overlapping point, the reaction of the slag primarily contributed to heat generation after the sulfate depletion peak. Na_2SO_4 had the most significant promotion effect on the slag reaction, whereas DEIPA significantly inhibited it. Under low-temperature curing conditions, all samples except that with Na_2SO_4 exhibited a substantial difference at the beginning and did not intersect with the sample containing quartz powder (Fig. A. 3).

Figure 15 illustrates the contribution of slag to the cumulative heat. It can be inferred that not only the hydration of the slag but also the hydration of the cement clinker is inhibited at the initial stage. The difference curves between the control groups with and without the addition of quartz powder indicate that the presence of slag at low temperatures hampered the hydration of the clinker. The additives had a smaller effect on the clinker during the early stage; however, their effect became apparent after 40 h of hydration. The inhibitory effect of DEIPA on the binder hydration was reduced, possibly owing to its promotion of aluminate hydration. By contrast, $Ca(NO_2)_2$ and TEA intensified the inhibition of cement clinker hydration. Figure 14a shows that the exothermic peak of the aluminates was essentially absent in the samples containing $Ca(NO_2)_2$ and TEA. We speculate that the synergistic effect of slag and TEA or $Ca(NO_2)_2$ led to the suppression of aluminate hydration. The presence of slag has been observed to inhibit cement hydration, potentially attributed to concentration differences in elements between cement and slag at a curing temperature of 5 °C. Furthermore, the addition of $Ca(NO_2)_2$ further inhibits aluminate hydration because of its excessive Ca^{2+} content [46]. The complex interaction between TEA and Ca^{2+} also hinders the formation of calcium hydrate crystals, further impeding aluminate hydration [26].

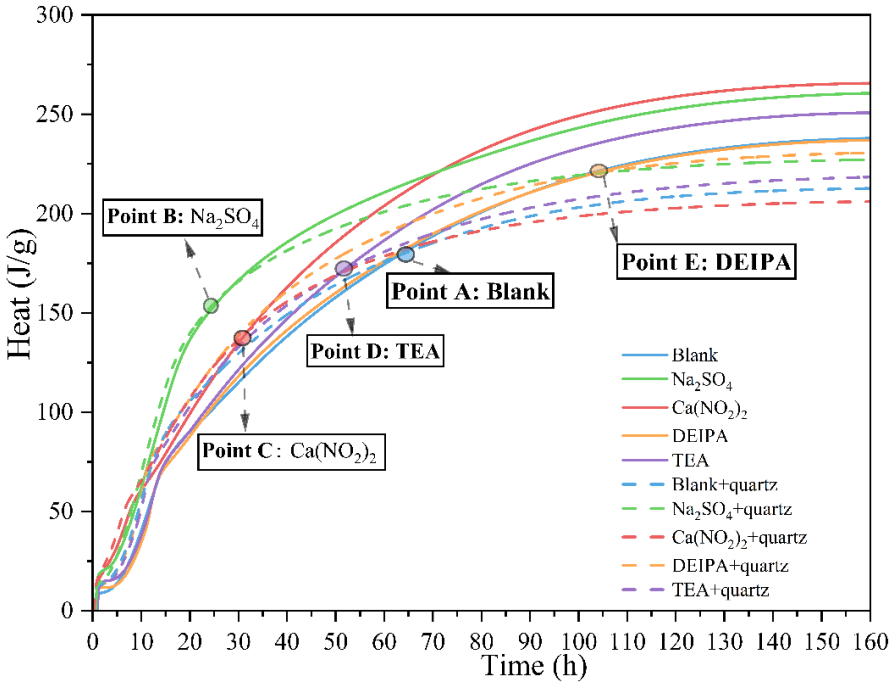

Fig. 14. The comparison in cumulative heat between samples treated with quartz powder and samples treated with slag at a curing temperature of 20 °C.

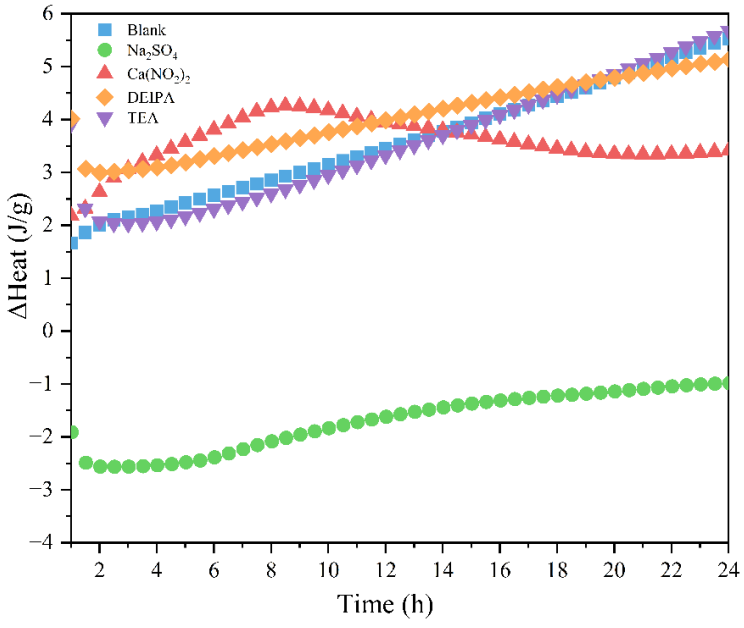

Fig. 15. The difference in cumulative heat between the slag-blended cement and quartz-blended cement at 5 °C.

4. Conclusions

In this study, the findings support the following conclusions:

1. At a curing temperature of 5 °C, the hydration of clinker in the samples treated with TEA and DEIPA may be inhibited at the initial stage, which may relate to the synergistic relationship between TEA, DEIPA, and slag. The presence of slag has been observed to inhibit cement hydration, which may be attributed to concentration differences in elements between cement and slag at a curing temperature of 5 °C. Furthermore, the complex interactions between the alkanolamines and Ca^{2+} hinder the formation of calcium hydrate crystals, further impeding aluminate hydration.
2. Na_2SO_4 promoted the slag-blended cement at 3 d, irrespective of the curing temperature. The promotion effects were caused by the acceleration of the clinker hydration and slag reaction. Although the strength development was strongly inhibited at 28 d at 20 °C, 1% of Na_2SO_4 is the best admixture at a curing temperature of 5 °C in this study; it could still promote strength to some degree at 5 °C, due to the relatively low reaction rate.
3. The effects of $Ca(NO_2)_2$ were sensitive to the curing temperature. At 20 °C, $Ca(NO_2)_2$ could promote the hydration of aluminates and the reaction of slag, and also promoted the strength development at 3 d. However, the synergistic relationship with slag suppressed clinker hydration in the initial stages and led to the inhibition of strength development at 5 °C.
4. At a low dosage of 0.02%, neither TEA nor DEIPA significantly enhanced strength development throughout the duration of the hydration period, irrespective of the curing temperature. At 20 °C, compared with the reference sample, TEA and DEIPA exhibited an accelerated hydration rate of alite but had no effect on the cumulative heat generated within the first day. After 2 d, TEA promoted the reaction of the slag, whereas DEIPA retarded it.
5. Although the addition of Na_2SO_4 can refine pore structure at the early stage because of the higher degree of hydration of the cement and slag, no densification of the pore structure occurred at 28 d, irrespective of the curing temperature. By contrast, TEA, DEIPA, and $Ca(NO_2)_2$ showed finer pore structures than the blank sample at 28 d, with $Ca(NO_2)_2$ showing this effect most prominently.

Acknowledgement

This work was supported by JCA 2023 Grant, JSPS KAKENHI Grant Number 21K04349, and JST SPRING Grant Number PH8D220001.

CRediT authorship contribution statement

Qi Zhai: Methodology, Investigation, Writing-Original Draft, Conceptualization. Kiyofumi Kurumisawa: Conceptualization, investigation, writing, reviewing and editing, supervision. Juhyuk Moon: validation, review, and editing.

Compliance with ethics guidelines

Qi Zhai, Kiyofumi Kurumisawa, and Juhyuk Moon declare that they have no competing financial interests or personal relationships that may have influenced the work reported in this study.

Appendix A: Figures

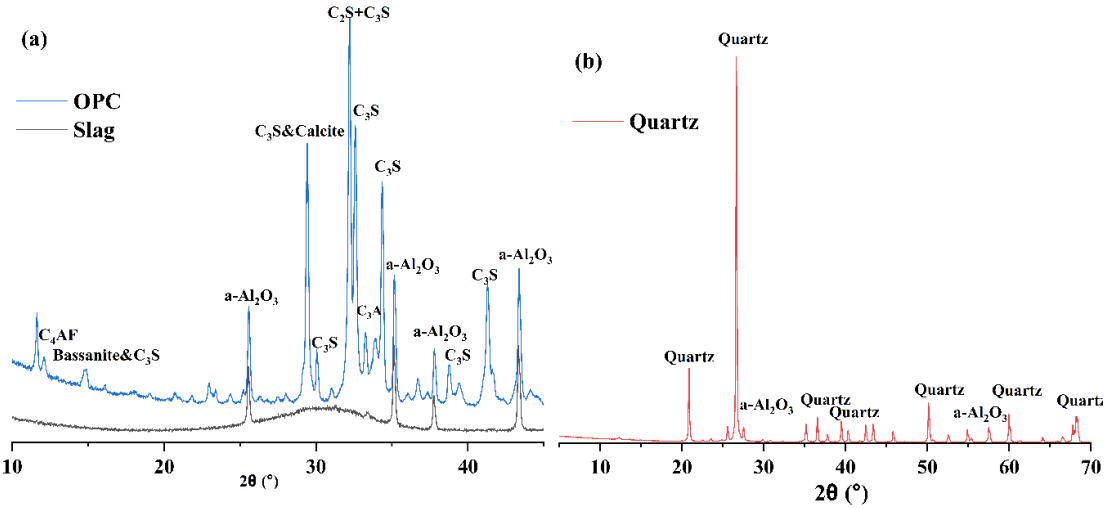

Fig. A. 1. XRD pattern of raw materials. a) OPC and slag; b) quartz powder.

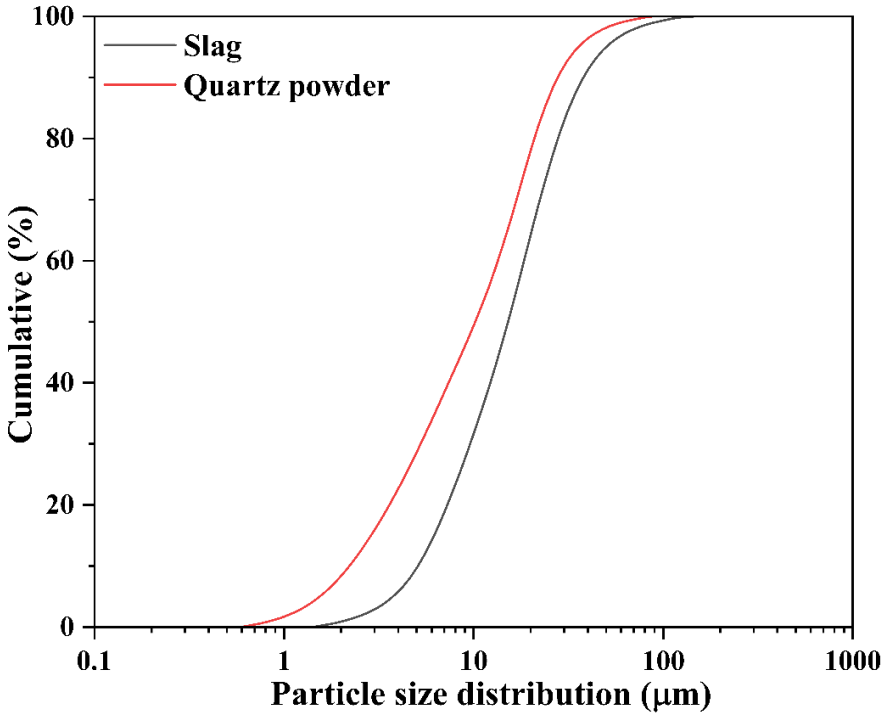

533 Fig. A. 2. The cumulative particle size distribution of the slag and quartz powder used in
534 this study.

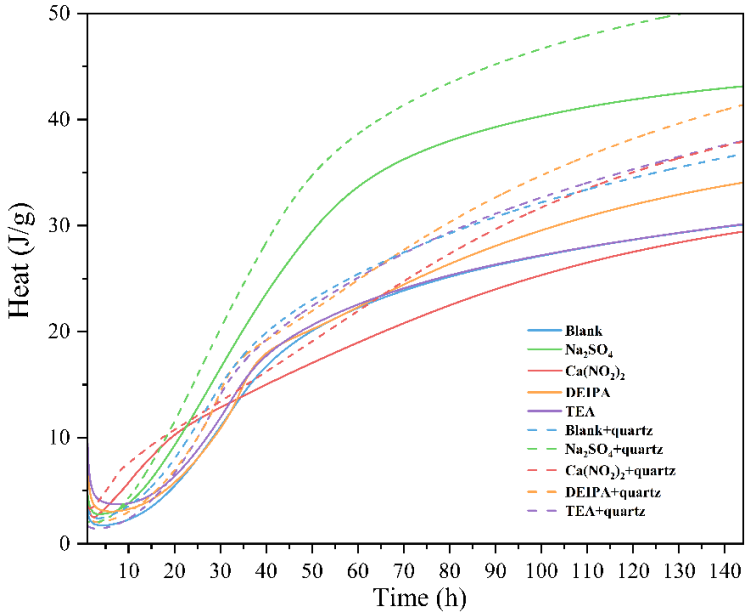

535

536 Fig. A. 3. The difference in cumulative heat between samples treated with quartz powder
537 and samples treated with slag at a curing temperature of 5 °C.

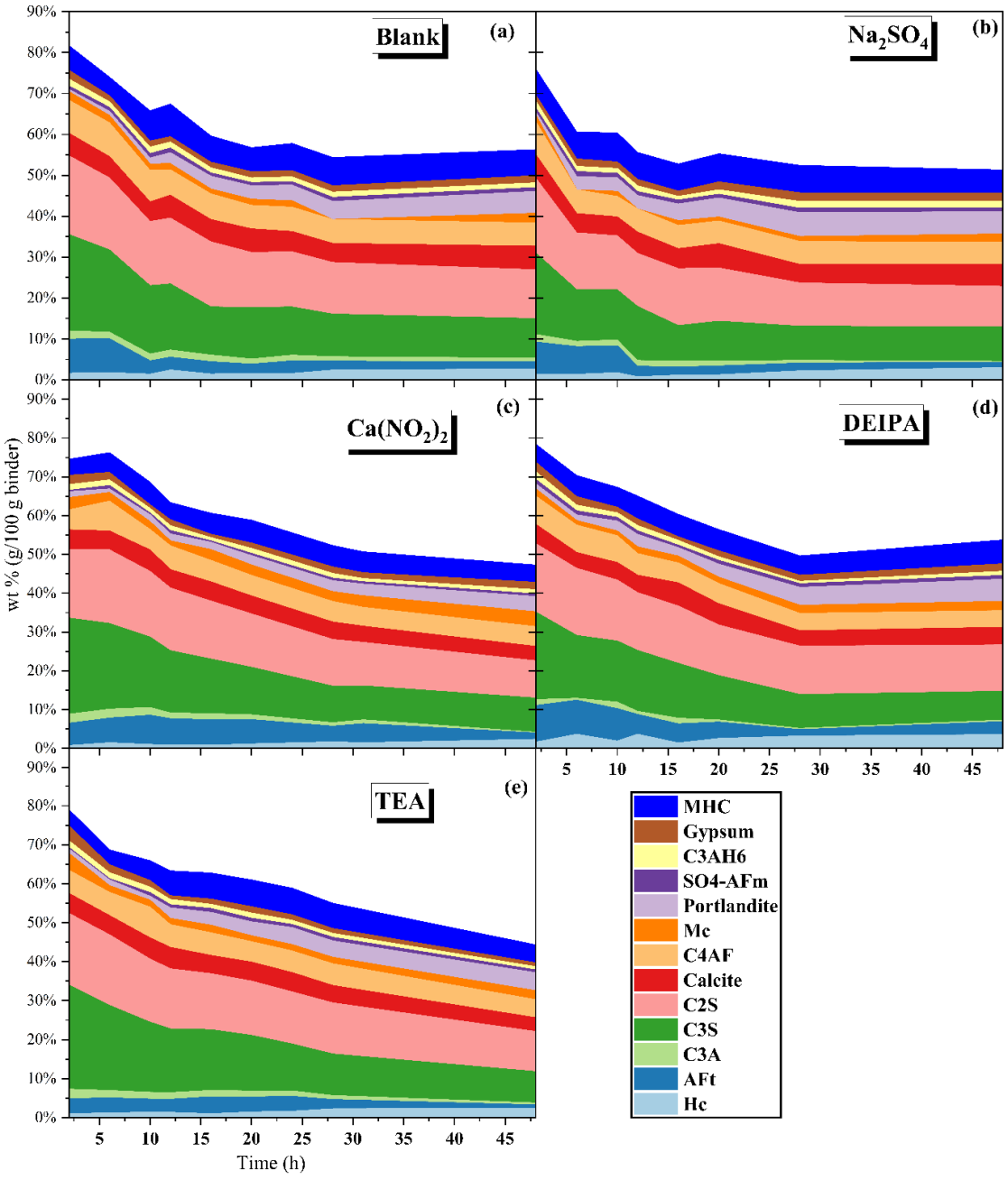

Fig. A. 4. The reaction process of the slag-blended cement cured at 20 °C by a combination of heat flow and XRD. a) Blank; b) Na_2SO_4; c) $Ca(NO_2)_2$; d) DEIPA; e) TEA.

Appendix B: Table

Table. B. 1 Amount of remaining clinker minerals at 20 °C.

Sample ID	Crossover point	Unreacted Clinker minerals (wt%)			
		C3S	C2S	C3A	C4AF
Blank	A(60hour)	7.38	10.2	0.04	5.02
Blank + Quartz		3.76	9.12	0	3.43
Na_2SO_4	B(28hour)	8.35	10.57	0.66	5.63
Na_2SO_4 + Quartz		6.79	8.54	0.2	2.83
$Ca(NO_2)_2$	C(31hour)	8.75	11.21	1	4.86
$Ca(NO_2)_2$ + Quartz		7.25	9.19	0.11	4.24
TEA	D(51hour)	6.32	9.7	0.3	3.93
TEA + Quartz		4.34	8.25	0	2.5
DEIPA	E(103hour)	3.46	7.59	0	1.24
DEIPA + Quartz		5.25	10.61	0.03	2.68

References

[1] G. Habert, S.A. Miller, V.M. John, J.L. Provis, A. Favier, A. Horvath, K.L. Scrivener, Environmental impacts and decarbonization strategies in the cement and concrete industries, Nat Rev Earth Environ. 1 (2020) 559–573. https://doi.org/10.1038/s43017-020-0093-3.

[2] J. Lehne, F. Preston, Chatham House Report Making Concrete Change Innovation in Low-carbon Cement and Concrete #ConcreteChange, n.d. www.chathamhouse.org.

[3] M. Schneider, M. Romer, M. Tschudin, H. Bolio, Sustainable cement production-present and future, Cem Concr Res. 41 (2011). https://doi.org/10.1016/j.cemconres.2011.03.019.

[4] L. Steger, S. Blotevogel, L. Frouin, C. Patapy, M. Cyr, Experimental evidence for the acceleration of slag hydration in blended cements by the addition of CaCl2, Cem Concr Res. 149 (2021) 2–10. https://doi.org/10.1016/j.cemconres.2021.106558.

[5] H.S. Lee, X.Y. Wang, L.N. Zhang, K.T. Koh, Analysis of the optimum usage of slag for the compressive strength of concrete, Materials. 8 (2015). https://doi.org/10.3390/ma8031213.

[6] J. Fu, A.M. Jones, M.W. Bligh, C. Holt, L.M. Keyte, F. Moghaddam, S.J. Foster, T.D. Waite, Mechanisms of enhancement in early hydration by sodium sulfate in a slag-cement blend – Insights from pore solution chemistry, Cem Concr Res. 135 (2020) 106110. https://doi.org/10.1016/j.cemconres.2020.106110.

[7] E. Gruyaert, N. Robeyst, N. de Belie, Study of the hydration of Portland cement blended with blast-furnace slag by calorimetry and thermogravimetry, J Therm Anal Calorim. 102 (2010). https://doi.org/10.1007/s10973-010-0841-6.

[8] A. Kunhi Mohamed, S.A. Weckwerth, R.K. Mishra, H. Heinz, R.J. Flatt, Molecular modeling of chemical admixtures; opportunities and challenges, Cem Concr Res. 156 (2022). https://doi.org/10.1016/j.cemconres.2022.106783.

[9] A.M. Rashad, Y. Bai, P.A.M. Basheer, N.B. Milestone, N.C. Collier, Hydration and properties of sodium sulfate activated slag, Cem Concr Compos. 37 (2013). https://doi.org/10.1016/j.cemconcomp.2012.12.010.

[10] X. Dai, S. Aydın, M.Y. Yardımcı, K. Lesage, G. de Schutter, Effect of ca(Oh)2 addition on the engineering properties of sodium sulfate activated slag, Materials. 14 (2021). https://doi.org/10.3390/ma14154266.

[11] J. Fu, M.W. Bligh, I. Shikhov, A.M. Jones, C. Holt, L.M. Keyte, F. Moghaddam, C.H. Arns, S.J. Foster, T.D. Waite, A microstructural investigation of a Na2SO4 activated cement-slag blend, Cem Concr Res. 150 (2021) 106609. https://doi.org/10.1016/j.cemconres.2021.106609.

[12] B. Mota, T. Matschei, K. Scrivener, Impact of sodium gluconate on white cement-slag systems with Na2SO4, Cem Concr Res. 122 (2019). https://doi.org/10.1016/j.cemconres.2019.04.008.

[13] B. Mota, T. Matschei, K. Scrivener, Impact of NaOH and Na2SO4 on the kinetics and microstructural development of white cement hydration, Cem Concr Res. 108 (2018). https://doi.org/10.1016/j.cemconres.2018.03.017.

[14] S. Joseph, J. Skibsted, Ö. Cizer, Hydration of polyphase Ca3SiO5-Ca3Al2O6 in the presence of gypsum and Na2SO4, Journal of the American Ceramic Society. 103 (2020) 6461–6474. https://doi.org/10.1111/jace.17321.

[15] L. Zhang, B. Chen, Hydration and Properties of Slag Cement Activated by Alkali and Sulfate, Journal of Materials in Civil Engineering. 29 (2017). https://doi.org/10.1061/(asce)mt.1943-5533.0001879.

[16] E. SAKAI, Y. UEDA, Y. AIKAWA, N. NITO, INFLUENCE OF CALCIUM NITRITE ON THE HYDRATION OF HIGH VOLUME SLAG CEMENT, Cement Science and Concrete Technology. 71 (2017). https://doi.org/10.14250/cement.71.62.

[17] A. Yoneyama, H. Choi, M. Inoue, J. Kim, M. Lim, Y. Sudoh, Effect of a nitrite/nitrate-based accelerator on the strength development and hydrate formation in cold-weather cementitious materials, Materials. 14 (2021). https://doi.org/10.3390/ma14041006.

601 [18] S. Yang, J. Wang, S. Cui, H. Liu, X. Wang, Impact of four kinds of alkanolamines
602 on hydration of steel slag-blended cementitious materials, Constr Build Mater. 131 (2017)
603 655–666. https://doi.org/10.1016/j.conbuildmat.2016.09.060.

604 [19] F. Zunino, K. Scrivener, Assessing the effect of alkanolamine grinding aids in
605 limestone calcined clay cements hydration, Constr Build Mater. 266 (2021).
606 https://doi.org/10.1016/j.conbuildmat.2020.121293.

607 [20] S. Ma, W. Li, S. Zhang, Y. Hu, X. Shen, Study on the hydration and microstructure
608 of Portland cement containing diethanol-isopropanolamine, Cem Concr Res. 67 (2015) 122–
609 130. https://doi.org/10.1016/j.cemconres.2014.09.002.

610 [21] Z. Xu, W. Li, J. Sun, Y. Hu, K. Xu, S. Ma, X. Shen, Research on cement hydration
611 and hardening with different alkanolamines, Constr Build Mater. 141 (2017) 296–306.
612 https://doi.org/10.1016/j.conbuildmat.2017.03.010.

613 [22] Y. Wang, L. Lei, X. Hu, Y. Liu, C. Shi, Effect of diethanolisopropanolamine and
614 ethyldiisopropylamine on hydration and strength development of Portland cement, Cem
615 Concr Res. 162 (2022). https://doi.org/10.1016/j.cemconres.2022.106999.

616 [23] K. Riding, D.A. Silva, K. Scrivener, Early age strength enhancement of blended
617 cement systems by CaCl2 and diethanol-isopropanolamine, Cem Concr Res. 40 (2010) 935–
618 946. https://doi.org/10.1016/j.cemconres.2010.01.008.

619 [24] X. ling Liao, H. Huang, F. qiang He, C. hui Yang, Microstructural characterization
620 of cement in the presence of alkanolamines, Mater Today Commun. 27 (2021).
621 https://doi.org/10.1016/j.mtcomm.2021.102386.

622 [25] Z. Lu, X. Kong, D. Jansen, C. Zhang, A comparative study of the effects of two
623 alkanolamines on cement hydration, Advances in Cement Research. 34 (2022).
624 https://doi.org/10.1680/jadcr.20.00063.

625 [26] Z. Lu, X. Kong, D. Jansen, C. Zhang, J. Wang, X. Pang, J. Yin, Towards a further
626 understanding of cement hydration in the presence of triethanolamine, Cem Concr Res. 132
627 (2020). https://doi.org/10.1016/j.cemconres.2020.106041.

628 [27] Y.R. Zhang, X.M. Kong, Z.C. Lu, Z.B. Lu, Z. Qing, B.Q. Dong, X. Feng, Influence
629 of triethanolamine on the hydration product of portlandite in cement paste and the mechanism,
630 Cem Concr Res. 87 (2016) 64–76. https://doi.org/10.1016/j.cemconres.2016.05.009.

631 [28] H. Tan, K. Nie, X. He, Y. Guo, X. Zhang, X. Deng, Y. Su, J. Yang, Effect of organic
632 alkali on compressive strength and hydration of wet-grinded granulated blast-furnace slag
633 containing Portland cement, Constr Build Mater. 206 (2019) 10–18.
634 https://doi.org/10.1016/j.conbuildmat.2019.02.028.

635 [29] H. Huang, X. Li, F. Avet, W. Hanpongpun, K. Scrivener, Strength-promoting
636 mechanism of alkanolamines on limestone-calcined clay cement and the role of sulfate, Cem
637 Concr Res. 147 (2021). https://doi.org/10.1016/j.cemconres.2021.106527.

638 [30] Y. Wang, L. Lei, X. Hu, Y. Liu, C. Shi, Effect of diethanolisopropanolamine and

639 ethyldiisopropylamine on hydration and strength development of Portland cement, Cem
640 Concr Res. 162 (2022). https://doi.org/10.1016/j.cemconres.2022.106999.

641 [31] O.R. Ogirigbo, L. Black, Influence of slag composition and temperature on the
642 hydration and microstructure of slag blended cements, Constr Build Mater. 126 (2016) 496–
643 507. https://doi.org/10.1016/j.conbuildmat.2016.09.057.

644 [32] J.S. Lumley, R.S. Gollop, G.K. Moir, H.F.W. Taylor, Degrees of reaction of the slag
645 in some blends with Portland cements, Cem Concr Res. 26 (1996).
646 https://doi.org/10.1016/0008-8846(95)00190-5.

647 [33] M. Ozturk, M. Karaaslan, O. Akgol, U.K. Sevim, Mechanical and electromagnetic
648 performance of cement based composites containing different replacement levels of ground
649 granulated blast furnace slag, fly ash, silica fume and rice husk ash, Cem Concr Res. 136
650 (2020). https://doi.org/10.1016/j.cemconres.2020.106177.

651 [34] J. Dai, Q. Wang, X. Lou, X. Bao, B. Zhang, J. Wang, X. Zhang, Solution calorimetry
652 to assess effects of water-cement ratio and low temperature on hydration heat of cement,
653 Constr Build Mater. 269 (2021). https://doi.org/10.1016/j.conbuildmat.2020.121222.

654 [35] G. Huang, D. Pudasainee, R. Gupta, W.V. Liu, Hydration reaction and strength
655 development of calcium sulfoaluminate cement-based mortar cured at cold temperatures,
656 Constr Build Mater. 224 (2019). https://doi.org/10.1016/j.conbuildmat.2019.07.085.

657 [36] S. Yang, J. Wang, S. Cui, H. Liu, X. Wang, Impact of four kinds of alkanolamines
658 on hydration of steel slag-blended cementitious materials, Constr Build Mater. 131 (2017)
659 655–666. https://doi.org/10.1016/j.conbuildmat.2016.09.060.

660 [37] Z. Xu, W. Li, J. Sun, Y. Hu, K. Xu, S. Ma, X. Shen, Research on cement hydration
661 and hardening with different alkanolamines, Constr Build Mater. 141 (2017) 296–306.
662 https://doi.org/10.1016/j.conbuildmat.2017.03.010.

663 [38] Q. Zhai, K. Kurumisawa, Effects of cation in sulfate chloride and nitrite on Ca(OH)2
664 activated ground granulated blast-furnace slag, Cem Concr Compos. 133 (2022).
665 https://doi.org/10.1016/j.cemconcomp.2022.104648.

666 [39] V. Kocaba, E. Gallucci, K.L. Scrivener, Methods for determination of degree of
667 reaction of slag in blended cement pastes, Cem Concr Res. 42 (2012).
668 https://doi.org/10.1016/j.cemconres.2011.11.010.

669 [40] P.T. Durdziński, M. ben Haha, S.A. Bernal, N. de Belie, E. Gruyaert, B. Lothenbach,
670 E. Menéndez Méndez, J.L. Provis, A. Schöler, C. Stabler, Z. Tan, Y. Villagrán Zaccardi, A.
671 Vollpracht, F. Winnefeld, M. Zając, K.L. Scrivener, Outcomes of the RILEM round robin on
672 degree of reaction of slag and fly ash in blended cements, Materials and Structures/Materiaux
673 et Constructions. 50 (2017). https://doi.org/10.1617/s11527-017-1002-1.

674 [41] X.M. Kong, Z.B. Lu, H. Liu, D.M. Wang, Influence of triethanolamine on the
675 hydration and the strength development of cementitious systems, Magazine of Concrete
676 Research. 65 (2013). https://doi.org/10.1680/macr.13.00015.

[42] Z. Zhang, G.W. Scherer, A. Bauer, Morphology of cementitious material during early hydration, Cem Concr Res. 107 (2018). https://doi.org/10.1016/j.cemconres.2018.02.004.

[43] Y. Zhang, L. Qiao, H. Yan, I. Zizak, P. Zaslansky, Y. Li, L. Qi, Y. Ma, Vaterite Microdisc Mesocrystals Exposing the (001) Facet Formed via Transformation from Proto-Vaterite Amorphous Calcium Carbonate, Cryst Growth Des. 20 (2020). https://doi.org/10.1021/acs.cgd.0c00259.

[44] K. Sanjiv Raj, M. Nirmala Devi, K. Palanisamy, V.K. Subramanian, Individual and synergetic effect of EDTA and NTA on polymorphism and morphology of CaCO3 crystallization process in presence of barium, J Solid State Chem. 302 (2021). https://doi.org/10.1016/j.jssc.2021.122026.

[45] F. Konrad, B. Purgstaller, F. Gallien, V. Mavromatis, P. Gane, M. Dietzel, Influence of aqueous Mg concentration on the transformation of amorphous calcium carbonate, J Cryst Growth. 498 (2018). https://doi.org/10.1016/j.jcrysgro.2018.07.018.

[46] Q. Zhai, K. Kurumisawa, Effect of accelerators on Ca(OH)2 activated ground granulated blast-furnace slag at low curing temperature, Cem Concr Compos. 124 (2021) 104272. https://doi.org/10.1016/j.cemconcomp.2021.104272.

Figure Captions

Fig. 1. Compressive strength of slag blended cement mortars containing chemical additives. a) cured at 5 °C; b) cured at 20 °C.

Fig. 2. The degree of reaction of slag and clinker up to 28 d by BSE. A) clinker cured at 5 °C, b) slag cured at 5 °C, c) clinker cured at 20 °C and d) slag cured at 20 °C.

Fig. 3. Relationship between compressive strength and reaction degree of the binder.

Fig. 4. Microstructure of slag-blended cement observed by BSE.

Fig. 5. XRD spectra of pastes treated with additives. a) 3 d cured at 5 °C; b) 3 d cured at 20 °C; c) 28 d cured at 5 °C and d) 28 d cured at 20 °C.

Fig. 6. Phase assemblage of samples treated with chemical additives. a) 3 d cured at 5 °C; b) 3 d cured at 20 °C; c) 28 d cured at 5 °C and d) 28 d cured at 20 °C.

Fig. 7. Pore structure of the pastes treated with chemical additives at 3 d. a) and b) pore size distribution of the samples cured at 5 °C; c) and d) pore size distribution of samples cured at 20 °C.

Fig. 8. Pore structure of the pastes treated with chemical additives at 28 d. a) and b) pore size distribution of the samples cured at 5 °C; c) and d) pore size distribution of samples cured at 20 °C.

Fig. 9. Relationship between compressive strength and capillary porosity.

Fig. 10. Morphology of the slag-blended cement at 3 d. a) Blank; b) Na_2SO_4; c) $Ca(NO_2)_2$; d)

714 DEIPA; e) TEA.

715 Fig. 11. The influence of TEA on the morphology of slag-blended cement cured at a) 5 °C at
716 3 d; b) 20 °C at 3 d; c) 5 °C at 28 d; d) 20 °C at 28 d.

717 Fig. 12. Effect of additives on the heat flow and cumulative heat of slag-blended cement a)
718 and b) 5 °C; c) and d) 20 °C.

719 Fig. 13. The influence of additives on the heat flow and cumulative heat of cement treated
720 with quartz powder a) and b) 5 °C; c) and d) 20 °C.

721 Fig. 14. The comparison in cumulative heat between samples treated with quartz powder and
722 samples treated with slag at a curing temperature of 20 °C.

723 Fig. 15. The difference in cumulative heat between the slag-blended cement and quartz-
724 blended cement at 5 °C.

725